DOI: 10.13009/EUCASS2017-318

Effect of the wing trailing-edge flaps and spoilers position on the jet-vortex wake behind an aircraft during takeoff and landing run

Yu. M. Tsirkunov [*†], *M. A. Lobanova* [*], *A. I. Tsvetkov* [**], *B. A. Schepanyuk* [**]

[*] *Baltic State Technical University, 1st Krasnoarmeiskaya str. 1, 190005 Saint Petersburg, Russia*
[**] *Centre of Applied Aerodynamics, Research Park, Saint Petersburg State University*
190000 Saint Petersburg, Russia
[†] *Corresponding author: tsrknv@bstu.spb.su*

Abstract

The large-scale vortex structure of flow in the near wake behind an aircraft during its run on a runway is investigated numerically. The geometrical aircraft configuration was taken close to a mid-range commercial aircraft like Boeing 737-300. It included all essential elements: a body (fuselage), wings with winglets, horizontal and vertical stabilizers, engine nacelles, nacelle pylons, inboard flap track fairings, leading-edge and trailing-edge flaps, and spoilers. Flaps and spoilers position corresponded to the takeoff and landing run conditions. Computational simulation was based on solving the Reynolds averaged Navier-Stokes equations closed with the Menter SST turbulence model. Patterns of streamlines, fields of the axial vorticity and the turbulent intensity, vertical and horizontal velocity profiles in the wake are compared and discussed for both run regimes. The flow model was preliminary tested for validity by comparison of the calculated velocity profiles behind a small-scaled aircraft model with those obtained in special wind tunnel experiments.

1. Introduction

An aircraft rolling on a runway during takeoff or landing generates a strongly disturbed and long-living airflow behind it, which is known as a vortex wake. Such a wake, particularly behind a large airliner, presents a serious danger for a following aircraft, and this limits a runway capacity. For the takeoff and landing safety it is critically important to predict the wake properties, particularly its large-scale vortex structure.

The jet-vortex wake flow behind aircrafts remains an important and interesting subject of investigation for several decades. It is caused by practical needs of effective air traffic control and flight safety, and by an academic interest to complicated and correlated fluid mechanics phenomena in the wake. A considerable attention was paid to a single wing-tip vortex structure [1], dynamics and stability of a vortex pair in atmosphere [2, 3], near-field and far-field flow behind an aircraft under cruise conditions [4, 5], ground effect on the vortex behaviour [6, 7], contrail formation in aircraft wakes [8], and many other aspects. The great majority of publications are devoted to the study of the wake properties for the cruising flight conditions. A variety of theoretical, computational and experimental techniques were developed and used for analysis and control of wake flows. Excellent reviews [9, 10, 11, 12, 13] give a comprehensive view on the subject and contain several hundred references. Recent activities and results obtained within the European 7th Framework Program (FP7) are presented in reports of WakeNet3 [14]. In spite of intensive investigations of commercial aircrafts wake vortex systems under the cruise conditions, much less attention has been paid to the wake flow structure when an aircraft runs on a runway during takeoff and landing. Only several papers are devoted to the wake flow during landing approach (e.g. [15]). Contrary to the cruising flight, leading-edge and trailing-edge flaps, and spoilers are deflected as prescribed by the mode requirements when an aircraft rolls on a runway. For example, all flaps and spoilers are fully extended during landing run. One might expect that flaps and spoilers create a variety of concentrated vortices which interact and merge with each other, and form together with the wing tip vortices a very complex heterogenous vortex structure in the wake. Besides, a runway, as a solid screen, can effect considerably on the development of a wake flow.

DOI: 10.13009/EUCASS2017-318

The present paper describes the results of computational simulation on developing the jet-vortex wake behind a running mid-range aircraft like Boeing 737 in the near wake flow field. Two different flap and spoiler positions corresponding to takeoff and landing run conditions are considered. The engines were taken as running, and the gas velocity, pressure and temperature at the exits of the exhaust nozzle and the bypass duct were obtained from preliminary thermodynamic calculations of the engine. The flow patterns, the vortex structure, the turbulence intensity, and the profiles of vertical and horizontal velocity are presented and discussed. For validation of the computational model, special wind-tunnel test experiments and numerical simulation for the small-scaled aircraft model were carried out, and the vertical velocity profiles were compared.

2. Aircraft configuration

The configuration of an aircraft for computational investigation of the jet-vortex flow in the wake was taken close to the mid-range airplane Boeing 737-300. The aircraft 3D geometrical model was designed using SolidWorks15. It included all essential elements: a body (fuselage), wings with winglets, horizontal and vertical stabilizers, engine nacelles, nacelle pylons, inboard flap track fairings, Krueger flaps, slats, trailing-edge flaps, flight and ground spoilers. The body length was 32.2 m, wing span with winglets was 31.2 m, body height and width in the middle part were 4.01 m and 3.76 m, respectively, wing dihedral was 6°, horizontal stabilizer span was 12.7 m, horizontal stabilizer dihedral was 7°, the angle between the root airfoil chord and the body centerline (setting angle) was +1°, the wing was geometrically twisted, and the setting angle for wing tip was -0.8°. The horizontal stabilizer had no geometrical twisting and its setting angle was -2°. Configuration and sizes of the engine were taken close to the turbofan engine CFM 56-3. The length of the engine nacelle was 4.0 m. The diameters of the annular exhaust duct and bypass duct outlets were 0.51 m and 0.76 m, and 1.04 m and 1.30 m, respectively.

Position of leading- and trailing-edge flaps and spoilers corresponded to two regimes: takeoff run and landing run. In both cases Krueger flaps and all slats were fully extended. The trailing-edge flaps were deflected at the angle of 15 and 40 degrees for takeoff and landing run, respectively. Flight and ground spoilers were in full-up position (they were raised at the angle of 40 and 60 degrees, respectively) only for landing run mode. Coordinates of airfoils in various wing cross-sections were taken from UIUC Airfoil Coordinates Database [16]. Aircraft sizes were taken from available open information sources [17]. The aircraft configuration for landing run is shown in Fig. 1.

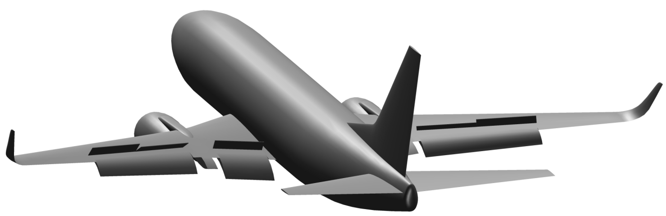

Figure 1: View of the aircraft model corresponding to the landing run conditions: leading- and trailing-edge flaps are fully extended, and flight and ground spoilers are fully raised.

3. Calculation domain, flow model and boundary conditions

Calculations were performed for two cases. At first, the flow over a small-scaled aircraft model was simulated numerically for experimental conditions in AT-11 wind tunnel, and the calculated and experimental vertical velocity profiles in the wake were compared to validate the flow model. Then a detail computational investigation of the near wake flow structure was performed for the actual-size aircraft with flaps and spoilers position corresponding to the takeoff and landing run. Specific features of the calculation domain and boundary conditions for flow simulation in the wind tunnel will be described in the next Section.

Here we describe the computational flow model used for the study of wake behind an actual-size aircraft. The calculation domain represented a rectangular parallelepiped (see Fig. 2) with 160.9 m length (5 body lengths), 46.7 m width (approx. a wing semi-span plus a body length), and 34.8 m height (approx. a body length). The forward point of the fuselage was located at the distance of 32.2 m (a body length) from the inflow boundary. Directions of coordinate axes are shown in Fig. 2 (z-axis is pointed in the opposite direction to the free stream velocity vector). The flow over an aircraft was assumed to be symmetric relative to the aircraft vertical centerline plane. The origin of the coordinate system was located in the plane of symmetry at the distance of 28.9 m from the inlet boundary (3.3 m ahead of the

DOI: 10.13009/EUCASS2017-318

body nose) and 2.6 m from the bottom boundary (runway). The outflow boundary is located at $z_{out} = -132.0$ m. An unstructured all boundary-fitted (including the aircraft surface) grid was designed using the ANSYS ICEM CFD soft. At first, the surface grid on the aircraft was constructed, then it was fixed and a volume grid was generated in the calculation domain. The total number of cells of the volume grid was approximately 11.2 million for the takeoff and 12.5 million for the landing conditions. The grid was refined towards the aircraft surface and in the wake area.

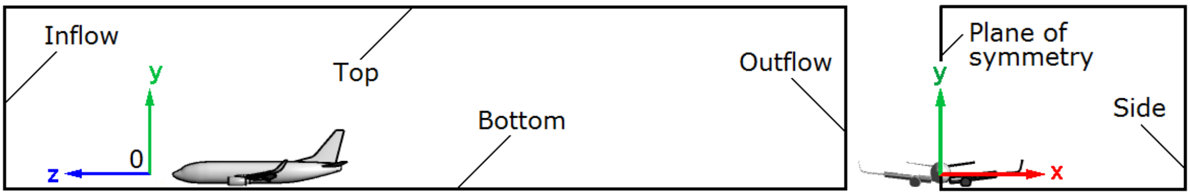

Figure 2: Side and front view of the calculational domain.

The Reynolds number of flow over an aircraft is of the order of 10^8, and hence the flow is turbulent. It was described by the Reynolds averaged Navier-Stokes (RANS) equations with Menter SST turbulence model. This flow model, as well as any other RANS-based model, does not allow to resolve the small-scale turbulent vortices, but it is quite applicable for studying the large-scale vortex structure of flow. Calculations were performed with the use of ANSYS soft.

At the inflow boundary, the velocity vector was taken as normal to it, and the temperature and total pressure were specified as follows: $T = 288.15$ K, $p_0 = 104357.6$ Pa. These values corresponded to the free stream velocity $V = 70$ m/s (it is equal to the speed of Boeing 737-300 on the runway during both takeoff and landing run) and static pressure $p = 101325$ Pa. Such a technique gave the entropy distribution at the inflow boundary very close to uniform (the difference between maximal and minimal values of the static entropy was much less than in the case of traditional specification of the velocity vector and the static pressure) that is physically correct. This technique is similar to that used in calculations of flow through a cascade of airfoils. The turbulence intensity was taken equal to 0.1 %. At the outflow boundary, the free stream pressure ($p = 101325$ Pa) was imposed, all other parameters were extrapolated from the calculation domain. The boundary conditions at the top and side boundaries were specified as 'opening' with the following velocity vector components and the temperature: $V_x = 0$; $V_y = 0$; $V_z = -70$ m/s, $T = 288.15$ K; the turbulent intensity was 0.1 %. Zero normal-velocity component together with the 'no-sleep wall' and adiabatic conditions were imposed at the aircraft surface. The bottom boundary (the runway) was considered as moving wall, at which the gas velocity components were taken as at the top or side boundary. All surfaces with 'wall' boundary condition were assumed to be smooth and adiabatic. The conditions of symmetry were specified at the plane of symmetry: the normal velocity (x-component) and all derivatives of thermodynamic parameters and y- and z-components of the velocity vector with respect to the normal direction (x-direction) were zero. These conditions are valid if the crosswind is absent. The engines were considered as running, and the gas velocity and temperature at the exit of the exhaust nozzle (V_1 and T_1) and the bypass duct (V_2 and T_2) were found from preliminary thermodynamic calculations of the turbofan engine CFM 56-3. Their values were the following: $V_1 = 517.37$ m/s, $T_1 = 883.36$ K, and $V_2 = 366.86$ m/s, $T_2 = 288.15$ K. The turbulence intensity was taken equal to 5 %. For simplicity, the gas constant and the ratio of specific heats for combustion products were taken identical to those for the air. It is rather rough assumption, but it allowed us not to simulate in detail the processes of mutual diffusion and mixing of the combustion products with the cocurrent air flow. The free stream velocity vector, the temperature and the pressure were taken as the initial conditions in the whole calculation domain for solving the time-dependent RANS-equations. Steady-state flow over an aircraft and in the wake was obtained as the limit of time-dependent solution.

4. Experimental and computational results for the flow over an aircraft model in the wind tunnel

Special experiments were carried out in AT-11 wind tunnel at the Center of Applied Aerodynamics of Saint Petersburg State University. The diameter and the length of the open test section were 2.25 m and 4 m, respectively. The aircraft model was made from plastic masterbatch on 3D printer in the scale 1/66 relative to the actual-size aircraft (its fuselage length was 0.5 m). The position of flaps and spoilers corresponded to the case of landing run. Engine nacelles were designed in the form of contoured ducts. The model was placed in the center of the test section near the glass screen (see. Fig. 3), and it was positioned at the distance of 16 mm from the screen surface and 188 mm from its leading edge.

PIV system was used for determining the velocity field in the model wake. This system included double-pulse Nd:YAG laser Quantel Twins CFR300, focusing lens Nikkor ED-180 mm with focal lenth 180 mm, cross-correlation

DOI: 10.13009/EUCASS2017-318

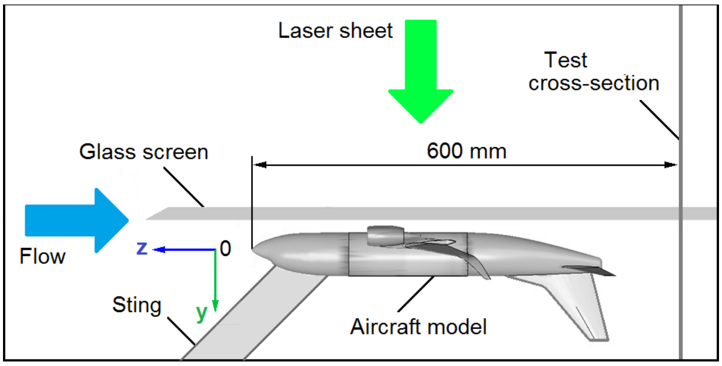

Figure 3: Arrangement of the aircraft small-scaled model relative to the screen and to the laser sheet of PIV system in experiments.

camera Videoscan-11002, timing sync processor, fog generator Magnum ZR33, three-axis traverse and control system. The camera had a matrix KAI-11002M with CCD size 36x24 mm and image resolution 4000x2673 px. Airflow seeding was carried out using a fog generator filled with a hydroglyceric blend 'MT Solid Fog Dense' giving 0.1...5 micrometers particle size. Time interval between two flashes of double-pulse laser was $\Delta t = 22$ microseconds. Laser sheet was directed downwards and oriented parallel to the model plane of symmetry. Planes of measurements were spaced 1 mm apart on one side of the model plane of symmetry. In every such plane, 200 instantaneous velocity fields were recorded by optical recording system, and the results were processed with ActualFlow software.

The free stream velocity in experiments was 20 m/s. The vertical velocity V_y (y-component of the velocity vector) as a function of x at $y = 0$ in the test cross-section located at the distance of 600 mm from the model nose (1/5 of the fuselage length behind an aircraft) is shown by solid circles in Fig. 4. The origin of the right-handed coordinate system (x, y, z) is positioned in the plane of symmetry at the distance of 39 mm from the screen and 50 mm from the model nose. Directions of y- and z-axes are shown in Fig. 3.

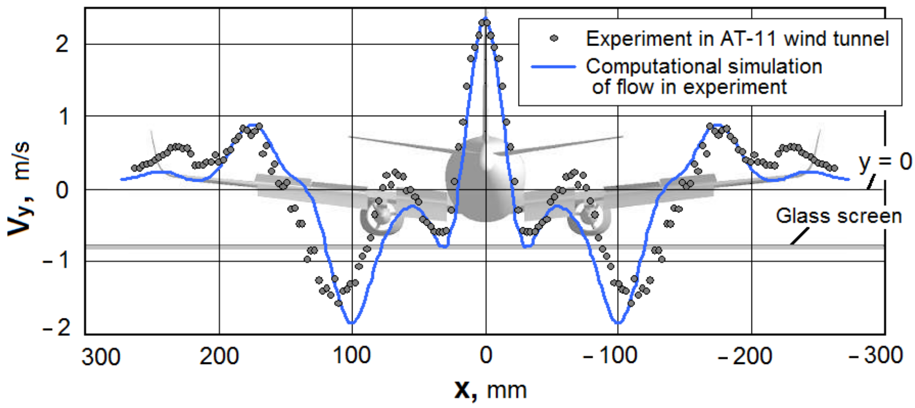

Figure 4: Comparison of the experimental and calculated vertical velocity profiles in the cross-section located at the distance of 600 mm downstream from the model nose (see Fig. 3) at $y = 0$.

Besides experimental measurements, the flow over a model and a screen in the test section was simulated numerically. A sting 1.5 mm thick was also taken into account. The calculational domain included areas from both sides of the screen. The grid was fitted to the model configuration. It was refined to the aircraft model and screen surfaces. The inflow conditions were taken similar to those for the actual size aircraft, but in contrast to them, the inflow velocity and the turbulence intensity were equal to 20 m/s and 0.85 %, respectively, and the tangential velocity at the screen surface was zero.

The plot of calculated V_y versus x at $y = 0$ in the test cross-section is shown by blue line in Fig. 4. As is seen, the distinction between experimental and calculated results is insignificant. Moreover, the calculated function $V_y(x)$ is within the confidence range of the experimental data. In other words, computed results are in good agreement with experimental ones if the PIV method error is taken into account. This means that the computational flow model fits rather well the purpose of the present study to investigate the large-scale vortex structure in the near wake behind an aircraft.

DOI: 10.13009/EUCASS2017-318

5. Results for a full-size aircraft and discussion

We consider and discuss the flow structure in the near field behind a full-size aircraft during its takeoff and landing run. The Krueger flaps and slats in both cases are fully extended, but positions of trailing-edge inboard and outboard flaps and spoilers are quite different. The trailing-edge flaps are at the position of 15 units for takeoff run and 40 units for landing run. The flight and ground spoilers do not work during takeoff, but they are fully raised during landing run. Results for both cases are presented in Figs. 5–10.

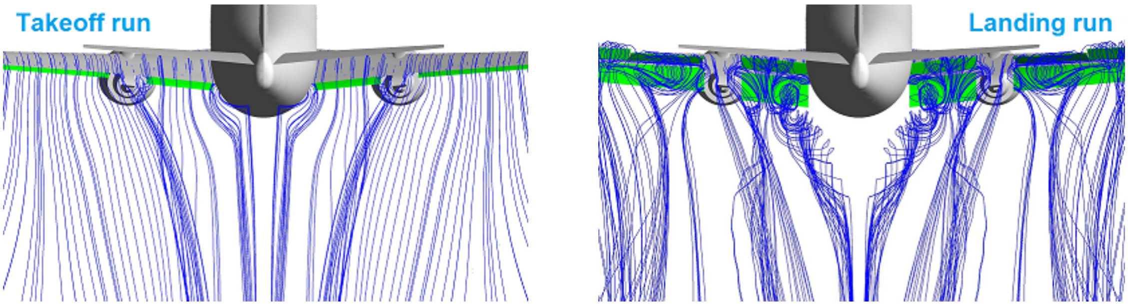

Figure 5: Fragments of back-up view of streamlines running off the wing, trailing-edge flaps and spoilers.

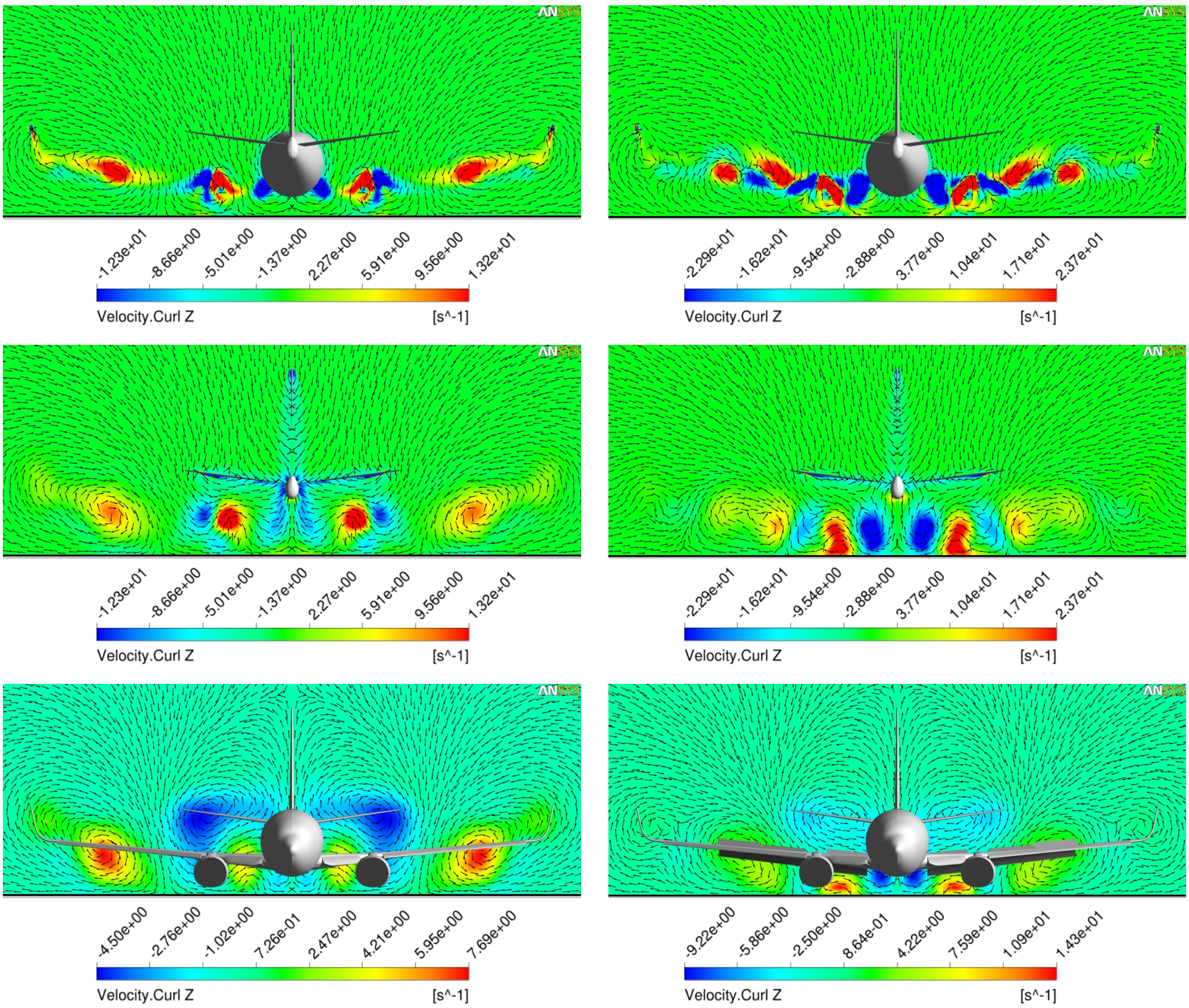

Figure 6: Axial vorticity fields and velocity vector patterns for takeoff run (left column) and landing run (right column) in different cross-sections: from top to bottom $z = -25$ m, -35 m, -55 m.

DOI: 10.13009/EUCASS2017-318

Patterns of streamlines (Fig. 5) demonstrate that the wake flow behind an aircraft during landing run is disturbed much higher than in the case of takeoff run. This is also evidenced by fields of axial vorticity (z-component of the vector Curl $\mathbf{V}$) and corresponding to them kinematic patterns (Fig. 6). Arrows show the direction of circulation flow. Scales of the axial vorticity under every picture applies only to its one half (containing the left part of the aircraft wing): to the left half for $z = -25$ m and -35 m, and to the right half for $z = -55$ m. Another half of every picture is obtained by mirror reflection, and it can be interpreted as the vorticity with the opposite sign. The aircraft image is given to indicate the vortices location relative to the wing. Right behind the wing ($z = -25$ m), the flow vorticity structure for both takeoff and landing run is rather complex: at least six axial vortices with opposite direction of rotation can be distinguished on each side of the vertical centerline plane. These vortices interact with each other downstream that results in their diffusion and merging, and already at the distance of approximately 1/2 of the fuselage length ($z = -55$ m) from the aircraft the kinematic pattern in each case differs qualitatively from that for $z = -25$ m. The scales of the axial vorticity at $z = -55$ m are local, and, as is seen, the range of the axial vorticity for landing run is twice wider than for takeoff run.

For detail quantitative analysis, it is most conveniently to consider the vertical velocity and the axial vorticity as functions of x at fixed y in different cross-sections. The results at $y = 0$ are shown in Figs. 7 and 8. We remind that $y = 0$ corresponds to the height of 2.6 m above the runway.

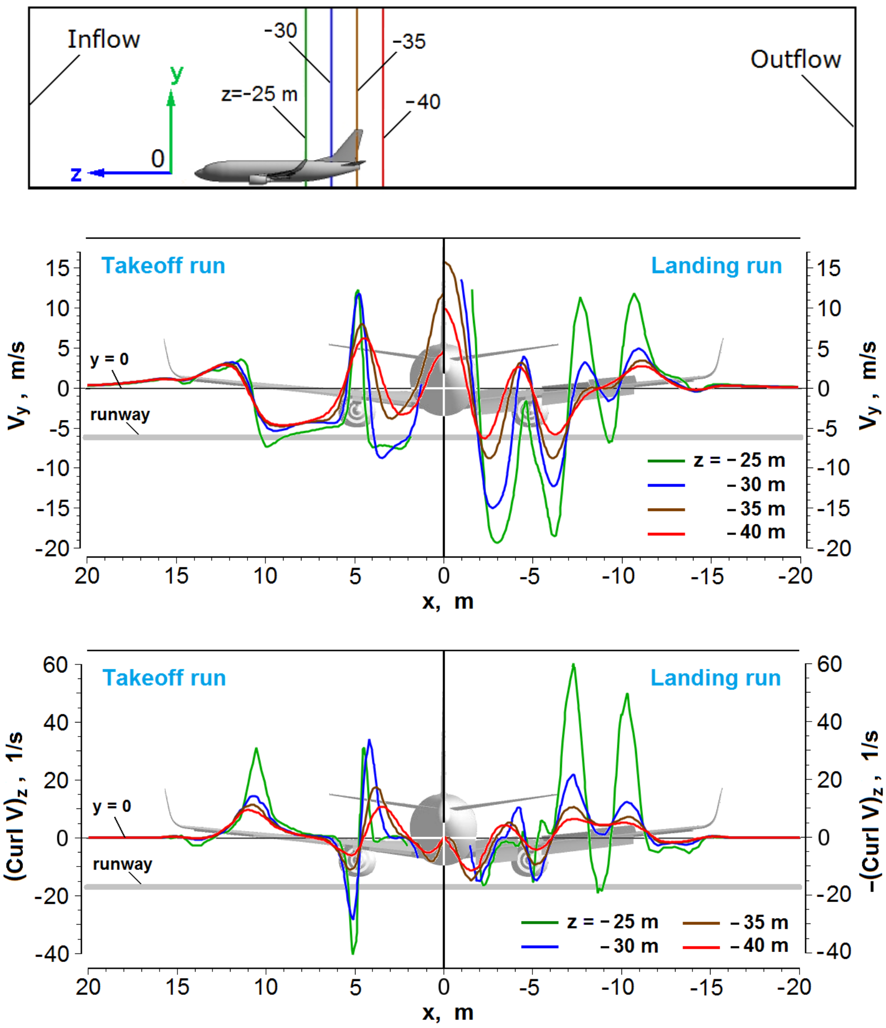

Figure 7: Vertical velocity (V_y) and axial vorticity (z-component of the vector Curl $\mathbf{V}$) distributions along x-axis at $y = 0$ in different cross-sections in the near wake.

Very strong difference in $V_y(x)$ and (Curl $\mathbf{V})_z(x)$ is observed for takeoff and landing run aircraft configurations. Right behind the wing, the velocity difference between minimal and maximal values reaches about 20 m/s for takeoff run and exceeds 35 m/s for landing run. This difference decreases downstream, and at the distance of three fuselage length ($z = -130$ m) it becomes about 5 m/s for both cases. For takeoff run, the axial vorticity in the near field

DOI: 10.13009/EUCASS2017-318

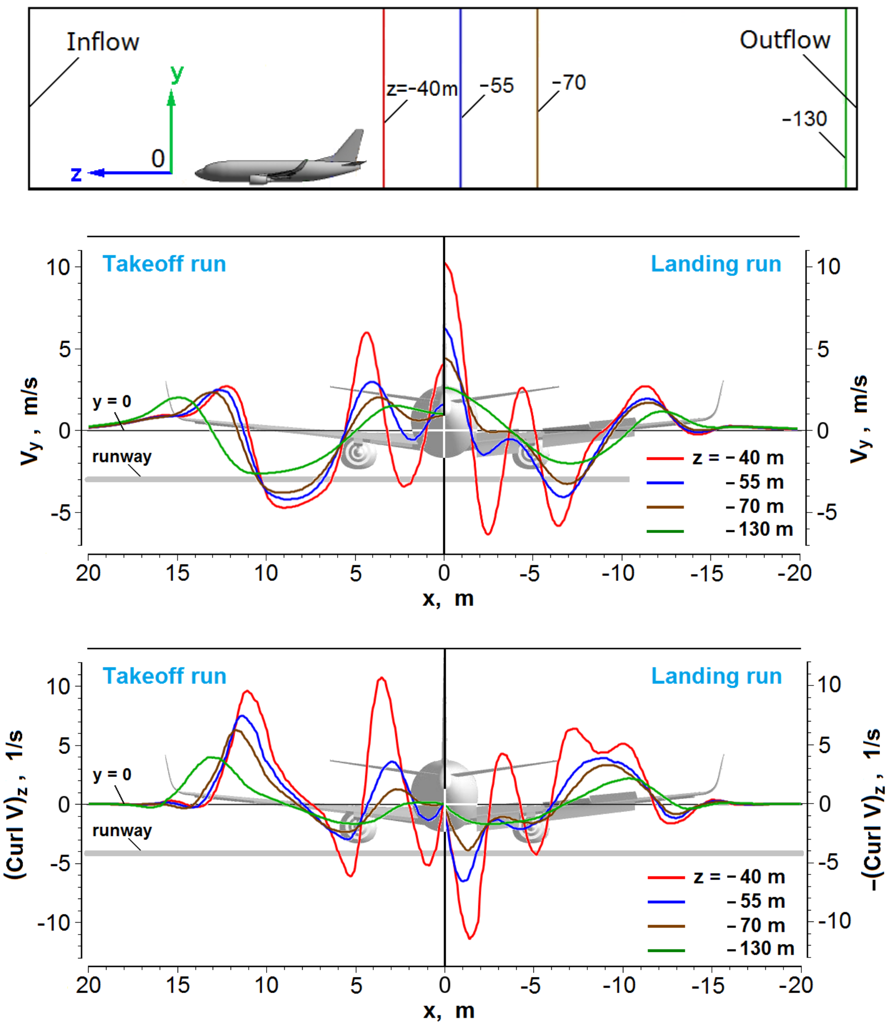

Figure 8: Vertical velocity (V_y) and axial vorticity (z-component of the vector Curl $\mathbf{V}$) distribution along x-axis at $y = 0$ in different cross-sections in the wake.

($z = -25$ m) is concentrated behind the inboard flap track fairings and the outer ends of outboard trailing-edge flaps. For landing run, the most intensive vorticity is localized behind the flight and ground spoilers. The intensity of vortices being rather high just behind an aircraft decreases quickly with distance from an aircraft. The maximal value of the axial vorticity decreases from approx. 40 s^{-1} for takeoff run and 60 s^{-1} for landing run (at $z = -25$ m) to approx. 4 s^{-1} and 2 s^{-1} (at $z = -130$ m). We call attention to the fact that profiles of $V_y(x)$ and $(\mathrm{Curl}\ \mathbf{V})_z(x)$ are correlated only partially because $(\mathrm{Curl}\ \mathbf{V})_z = \partial V_y/\partial x - \partial V_x/\partial y$ and hence it is determined not only by $V_y(x)$, but also by $V_x(y)$. It should be particularly emphasized that profiles of the vertical velocity and fields of the axial vorticity in both discussed here cases (takeoff and landing run) differ qualitatively from those for a cruising flight [18], when only two circulation flows with opposite rotation are generated by the wing on each side from the plane of symmetry. These distinctions are caused by several reasons: the aircraft speed, the aircraft angle of attack, the flaps and spoilers position, and the reflection effect of a runway on the wake flow. The present study shows that the last two effects play a dominant role in formation of the wake flow vortex structure when an aircraft rolls on the runway during takeoff and landing.

It is interesting to consider along with the vertical velocity V_y also the horizontal velocity V_x in the wake. In Fig. 9, plots of V_x versus x at $y = -2.4$ m are shown at various z. This value of y corresponds to the distance of 0.2 m from the runway, so that it is very close to the runway but out of the flow boundary layer. It is seen that the difference between maximum and minimum of V_x at $z = -30$ m is about 30 m/s for landing run that is three times greater than for takeoff run. This difference decreases downstream and at approx. $z = -55$ m it becomes less than that for takeoff run. We note that during landing run the flow horizontal velocity in the periphery of the near field (approx. from $z - 30$ m to -40 m) is directed to the plane of symmetry. It means the appearance of a weak vortices which are drawn in the wake from outside.

DOI: 10.13009/EUCASS2017-318

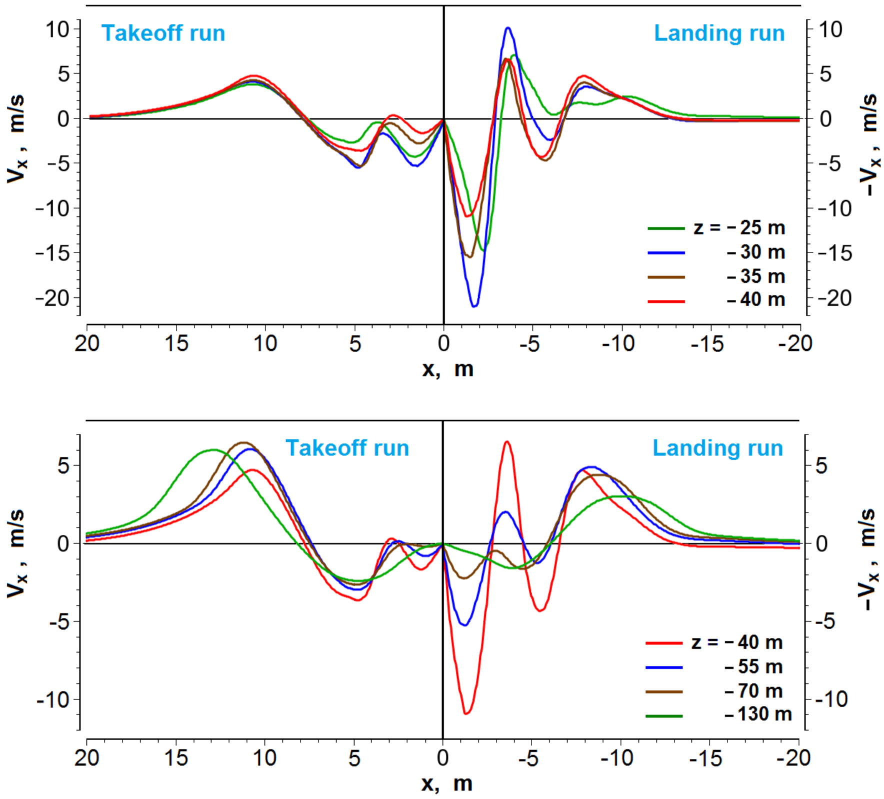

Figure 9: Horizontal velocity (V_x) distribution along x-axis at $y = -2.4$ m (0.2 m above the runway) in different cross-sections in the near wake.

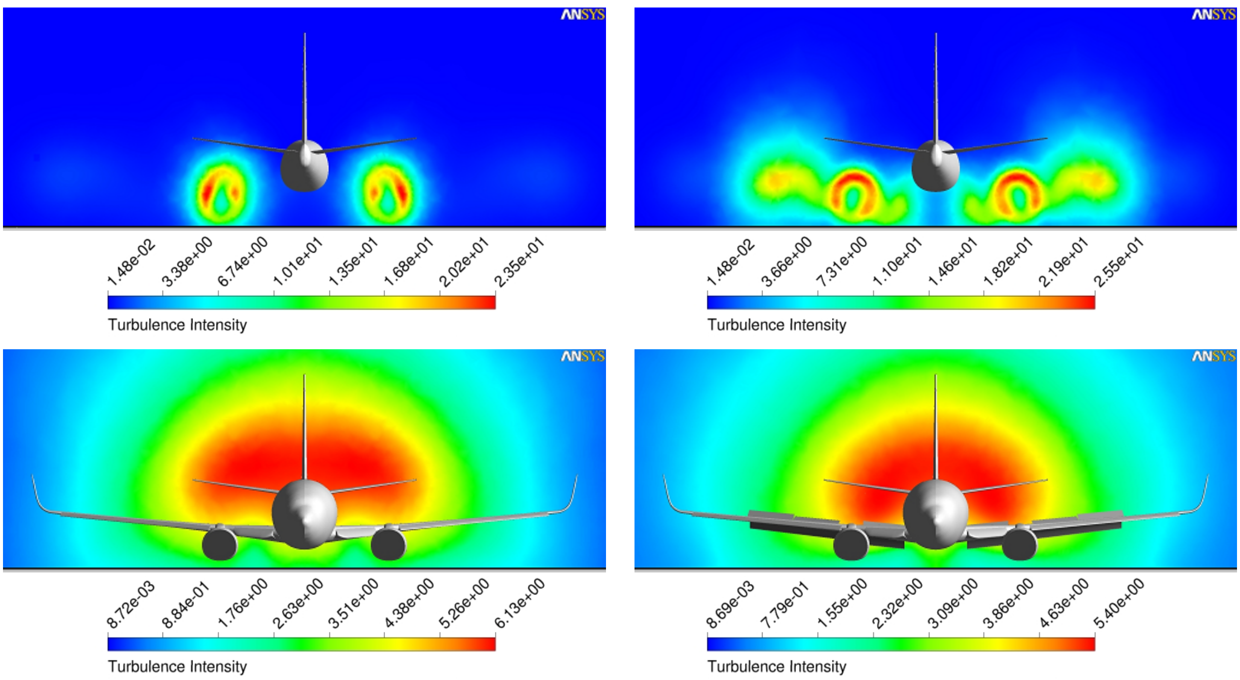

Figure 10: Field of turbulence intensity (%) for takeoff run (left column) and landing run (right column) in cross-sections $z = -30$ m (top) and $z = -130$ m (bottom). Scale under every picture is local.

Another flow parameter which is of great importance in the considered problem is the turbulence intensity. Fields

DOI: 10.13009/EUCASS2017-318

of the turbulence intensity in two cross-sections right behind an aircraft ($z = -30$ m) and at a distance of three fuselage lengths from the aircraft ($z = -130$ m) are shown in Fig. 10. It is clearly seen that high level of the turbulence intensity in the wake is caused by engine jets where the intensity reaches approx. 25 % at $z = -30$ m for both takeoff and landing run, and it decreases substantially downstream. It is interesting to note that the turbulence intensity at the periphery of the calculational domain becomes even less than in the inflow.

6. Conclusion

Computational simulation of the large-scale vortex structure of flow in the near wake behind a mid-range aircraft like Boeing 737-300 was performed in two cases: for takeoff and landing run. Flow fields of various parameters and kinematic flow patterns were obtained and analyzed in detail. The position of trailing-edge flaps and ground and flight spoilers was different for takeoff and landing run conditions. Calculations were based on solving the Reynolds averaged Navier–Stokes equations with the Menter SST turbulence model. The flow model was preliminary tested for validation by comparison of computed results with the experimental data obtained in the wind tunnel.

The present results show that the large-scale vortex structure of flow behind an aircraft running on a runway during takeoff or landing differs essentially from that in cruising flight of the same aircraft [18]. Flow over trailing-edge flaps and spoilers is accompanied by formation of numerous vortices in the wake, and their interaction with each other and with the wing-tip vortices result in a very complex vortex structure. Axial vorticity and transverse velocity distributions in the wake have several maxima and minima. The most important features of the wake flow are sum up below.

The greatest difference between maximal and minimal vertical velocity in the wake at a distance of 2.6 m above the runway (it corresponds to the aircraft nose position over the runway) takes place immediately behind a wing. This difference reaches 20 m/s for takeoff run and exceeds 30 m/s for landing run. It decreases downstream rapidly and becomes about 5 m/s at a distance of 3 fuselage lengths behind the aircraft for both takeoff and landing run. The last value is four times smaller than that in the case of a cruising flight [18].

The large-scale vortex structure and the field of the axial vorticity $(\mathrm{Curl}\,\mathbf{V})_z$ are well correlated. However the contribution of this vorticity component into the total vorticity Curl **V** is very small: it is 2 orders of magnitude smaller than the contribution of x- and y-components of Curl **V** which are caused by the engine jets.

The transverse horizontal velocity V_x as a function of x (distance from the plane of flow symmetry) was studied at a height of 0.2 m above the runway. The function $V_x(x)$ was found to be essentially non monotonic. For the case of landing run this velocity immediately behind the wing can reach 20 m/s in the direction towards the plane of flow symmetry and then it becomes about 10 m/s in the opposite direction, whereas for the case of takeoff run the velocity magnitude reaches only 5 m/s in each direction. It should be noted that in the case of landing run a weak transverse horizontal velocity directed toward the plane of symmetry appears at the periphery of flow. It can be interpreted as the injection of an ambient air into the wake and formation of a weak outer axial vortex. This phenomenon is absent in the case of takeoff run.

The highest turbulence level in the wake is observed immediately behind a wing. The turbulence intensity here is approximately 25% for both run modes, and it relatively slowly decreases downstream. Engine jets make the crucial contribution to turbulence generation in the wake whereas the role of the vortex sheet is very small.

The present results show that the length of the vortex wake behind a running aircraft which is really hazard to the following aircraft is much less than in the case of a cruising flight. However the problem is in the fact that the flight corridor is much wider than the area of a runway and, hence, aircrafts can be much easier moved apart in the sky than on the ground, and this limits the runway capacity.

Acknowledgements

The present study was supported by the Russian Foundation for Basic Research through grant No. 15-08-07965. The authors also wish to thank PhD student V. Gabdylkhakova for computer development of PIV measurements.

References

[1] Devenport W.J., Rife M.C., Liapis S.I., Follin G.J. 1996. The structure and development of a wing-tip vortex. *J. Fluid Mech.*, Vol. 312: 67-106.

[2] Widnall S.E. 1975. The structure and dynamics of vortex filaments. *Ann. Rev. Fluid Mech.*, Vol. 7: 141-165.

[3] Devenport W.J., Vogel C.M., Zsoldos J.S. 1999. Flow structure produced by the interaction and merger of a pair of co-rotating wing-tip vortices. *J. Fluid Mech.*, Vol. 394: 357-377.

[4] Stumpf E., Rudnik R., Ronzheimer A. 2000. Euler computation of the near-field wake vortex of an aircraft in take-off configuration. *Aerosp. Sci. Technol.*, Vol. 4: 535-543.

[5] Robins R.E., Delisif D.R. 1997. Numerical simulations of three-dimensional trailing vortex evolution. *AIAA Journal*, Vol. 35, No. 9: 1552-1555.

[6] Zheng Z.C., Ashf R.L. 1996. Study of aircraft wake vortex behavior near the ground. *AIAA Journal*, Vol. 34, No. 3: 580-589.

[7] Corjon A., Poinsot T. 1997. Behavior of wake vortices near ground. *AIAA Journal*, Vol. 35, No. 5: 849-855.

[8] Paoli R., Helie J., Poinsot T. 2004. Contrail formation in aircraft wakes. *J. Fluid Mech.*, Vol. 503: 361-373.

[9] Spalart P.R. 1998. Airplane trailing vortices. *Ann. Rev. Fluid Mech.*, Vol. 30: 107-138.

[10] Rossow V.J. 1999. Lift-generated vortex wakes of subsonic transport aircraft. *Progress in Aerospace Sciences*, Vol. 35: 507-660.

[11] Gerz T., Holzapfel F, Darracq D. 2002. Commercial aircraft wake vortices. *Progress in Aerospace Sciences*, Vol. 38: 181-208.

[12] Breitsamter C. 2011. Wake vortex characteristics of transport aircraft. *Progress in Aerospace Sciences*, Vol. 47: 89-134.

[13] Chernyshev S.L., Gaifullin A.M., Sviridenko Yu.N. 2014. Civil aircraft vortex wake. TsAGI's research activities. *Progress in Aerospace Sciences*, Vol. 71: 150-166.

[14] < http://www.wakenet.eu >.

[15] Stephan A., Holzapfel F., Misaka T. 2014. Simulation of aircraft wake vortices during landing with decay enhancing obstacles. *Proc. of 29th Congress of the Int. Council of the Aeronautical Sciences (ICAS 2014)*, Paper No. 0796.

[16] http://www.ae.illinois.edu/m-selig/ads/coord database.html

[17] http://www.b737.org.uk/

[18] Lobanova M.A., Tsirkunov Yu.M. 2012. Numerical simulation of a jet-vortex wake behind a cruise aircraft. *ECCOMAS 2012 – European Congress on Computational Methods in Applied Sciences and Engineering*, e-Book Full Papers: 6909-6922.